Production and Characterization of a Hybrid Polymer Matrix Composite

Gökhan Açıkbaş,[1] **Selçuk Özcan**,[2] **Nurcan Çalış Açıkbaş**[3]
[1]*Vocational School, Metallurgy Program, Bilecik S.E. University, Bilecik, Turkey*

[2]*Department of Chemical and Process Engineering, Bilecik S.E. University, Bilecik, Turkey*

[3]*Department of Metallurgical and Materials Engineering, Bilecik S.E. University, Bilecik, Turkey*

The aim of this study was to develop low cost hybrid composites with enhanced mechanical properties by the addition of industrial wall tile and glass fiber wastes into epoxy resin. This process not only reduces the production cost, but also helps to eliminate solid wastes. The detailed characterization of waste particulate fillers was performed by scanning electron microscopy, X-ray diffraction, X-ray fluorescence, laser diffraction, and He gas picnometer techniques. The effects of the ceramic particulates to glass fiber ratio and the particle size of the waste materials on the physical and mechanical properties were determined with a fixed polymer to filler ratio of 40:60. The density, three point bending strength, impact resistance and hardness of the hybrid composites were measured. The results indicated that when the filler particle size increased, the bulk density almost remained unchanged, and the bending strength and impact resistance decreased, while the hardness and flexural modulus were almost constant. Because of the weak matrix-reinforcement interphase, mechanical properties deteriorated with the increasing amount of waste glass fiber and better mechanical properties were achieved with the use of finer particles. As a result of incorporation of industrial wastes such as ground ceramic wall tile and glass fiber instead of expensive fillers, low cost reinforcement of the hybrid epoxy matrix composites was achieved. **POLYM. COMPOS., 39:4080–4093, 2018.** **© 2017 Society of Plastics Engineers**

INTRODUCTION

Hybrid composites are the materials made by incorporating two or more different types of reinforcing components in a matrix towards a synergistic improvement of properties. The hybrid reinforcement is expected to provide a performance that cannot be obtained with a single type of reinforcement. Hybrid composite approach can bring about a reduction in the production cost by the proper selection of reinforcement materials, for instance, replacing high quality, high cost carbon fibers without seriously impairing the required mechanical properties of the composite. A compromise between performance and cost should be observed in the material design [1–3].

In general, industrial wastes can be used as low cost reinforcements in hybrid composites provided that the mechanical and other property requirements of the finished product are met. Ease of manufacturing is also a desired advantage [4]. In the literature there exist efforts to employ glass, ceramic and porcelain ware and gypsum fiber production wastes, metallurgical, foundry and blast furnace slags, red mud, fly ash, flue dust, carbon black waste, and waste rubber as fillers for the reinforcement of polymer matrix materials [5–20]. For example, Ahmed et al studied the development of natural rubber hybrid composites reinforced with marble sludge/silica and marble sludge/rice husk derived silica. The results indicated that hybrid composites containing marble sludge/silica and marble sludge/rice husk derived silica as fillers showed better mechanical and swelling properties as compared to the use of marble sludge alone as filler [21]. Thwe and Liao studied the hydrothermal aging resistance and the fatigue behavior of bamboo fiber reinforced polypropylene composite (BFRP) and bamboo–glass fiber reinforced polypropylene hybrid composite (BGRP) under cyclic tensile load. The results showed that tensile strength and elastic modulus of both types of samples showed moderate reduction after aging for 6 months at 25°C, but they were reduced considerably after aging at 75°C for 3 months. Moisture absorption and tensile strength degradation are suppressed when maleic anhydride polypropylene was used as a coupling agent. BGRP composites had better fatigue resistance than BFRP composites [22]. Haneef et al. studied hybrid polymer matrix composites for biomedical applications. In their study high density polyethylene was used as the matrix and TiO_2 and Al_2O_3

Correspondence to: G. Açıkbaş; e-mail: gokhan.acikbas@bilecik.edu.tr
Contract grant sponsor: Bilecik Seyh Edebali University, Scientific Research Project; contract grant number: 2014-01.BİL.03-03.
DOI 10.1002/pc.24471
Published online in Wiley Online Library (wileyonlinelibrary.com).

particles were used in varying amounts as the reinforcements. It was observed that the mechanical and tribological properties were improved appreciably with the inclusion of the reinforcements, and the hybrid composites obtained carried the potential to be employed as materials for bone fixation plates, hip joint replacement, bone cement and bone graft [23]. Ashori produced polypropylene matrix hybrid composites reinforced with waste newspaper fiber and poplar wood flour. The mechanical and thermal properties, and the microstructure were investigated and it was found that tensile and flexural modulus increased with the addition of reinforcements. Microscopy examinations showed that the composite with a coupling agent enhanced the fiber-matrix interaction [5]. Sanjay and Yogesha studied the mechanical properties of Jute/E-Glass fiber reinforced epoxy hybrid composites. The properties of this hybrid composite were determined by tensile, flexural, impact, and inter laminar shear strength tests conducted according to the ASTM standards. The result of the test showed that hybrid composite of jute/E-glass fiber had far better properties than that of jute fiber composite [24]. Valente et al. produced hybrid thermoplastic composites from wood flour and recycled glass fibers which were manufactured via a two-step process involving a kinetic mixer and a compression molding machine. The flexural modulus and hardness were found to increase as a function of increasing wood flour and glass fiber content. However, the flexural strength and screw withdrawal resistance decreased with increasing wood flour content, even though a positive effect of the addition of glass fibers was detected [25].

Ceramic solid wastes are classified as non–hazardous industrial wastes the majority of which are formed during the ceramic processing as the discarded semi-finished products that cannot be further processed, or is over process recycling limits. Ceramic tiles, sanitary ware, tableware, fired clay products, electrical porcelain; refractories that are broken or defective beyond commercialization as well as accumulated ceramic plant dust, and ceramic sludge constitute examples of ceramic solid wastes. These waste materials are known to find use in industrial applications like blending with cement [26].

Solid wastes of ceramic plants includes fired vitrified product wastes amounting to an estimated 600 ton/year in Turkey. Since the land fill tax rate is £2.5 per tone, recycling for other industrial uses could be preferred [27]. Moreover, the use of waste ceramic wall tile and glass fiber has economical and ecological benefits on its own accord. Simplicity of the casting method for the preparation of hybrid composites is another advantage giving way to low fixed capital, and production costs.

Although there have been numerous studies on hybrid composites, there is no reference available related to the use of waste wall tile powder and glass fiber fillers in epoxy matrix hybrid composites. In this study, the fiber and particle reinforcing characteristics of waste glass fiber, waste wall tile particulates was exploited, respectively, in epoxy resin. The effects of wall tile particulates to glass fiber ratio, and the particle size of wastes on the mechanical and the physical properties were determined. The study also carries the advantage of reuse of wastes as a cheap source of raw materials.

FIG. 1. Representative image of as-received state of the glass fiber waste. [Color figure can be viewed at wileyonlinelibrary.com]

MATERIALS AND METHODS

Characterization of Wastes

The matrix material comprises epoxy resin (EpoxAcast690) and hardener which was supplied from Smooth-On Limited, Canada. The mixing ratio of the epoxy and hardener was 73:27 by weight. Wall tile waste was obtained from a local ceramic tile plant, in Bilecik, Turkey and waste glass fiber was supplied from Şişecam Glass Fiber Company, Gebze, Turkey. The as-received state image of the glass fiber waste that was formed during the production of chopped strand glass fibers is shown in Fig. 1. Although the glass fiber waste had higher aspect ratio in the as-received state than the ground state, since the aim of this study was the use of maximum filler content, the glass fiber should be ground to provide efficient mixing/homogeneous mixture. Otherwise, the glass fiber content would be low in the polymer matrix. Therefore, both waste materials were ground with a Fritsch Vibrating Cup Mill Pulverisette 9 for 2 min at 900 rpm. The ground waste was dry sieved for 5 min with Fritsch Vibratory Sieve Shaker Analysette 3 Spartan separated to particle size ranges of below 90 μm, 90–150 μm, and 150–300 μm.

The waste materials were characterized as follows. The theoretical density of the wastes was measured by Micromeritics Accupyc II 1340 model He-gas pycnometer. Theoretical densities of the glass fiber and wall tile powder were 2.61 gr/cm^3 and 2.54 gr/cm^3, respectively. Secondary electron scanning electron microscopy images of waste materials were taken with Zeiss Supra 40 VP FEG-SEM. The types of phases were determined by

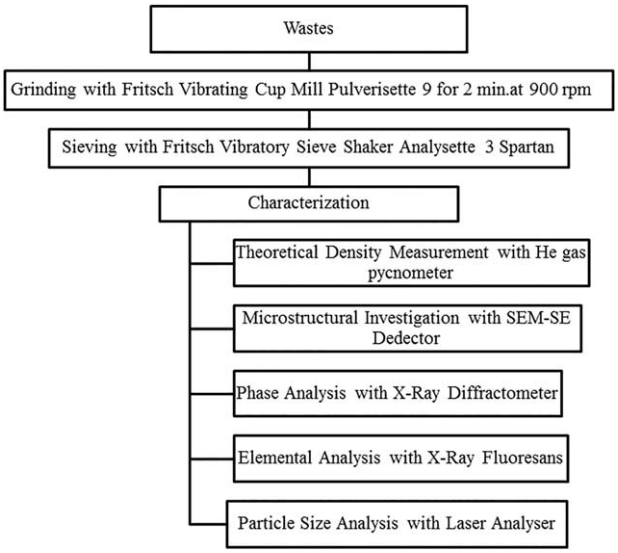

FIG. 2. Schematic presentation of waste preparation and characterization.

means of X-ray diffraction analyses (XRD-Panalytical, Empyrean with Cu-Kα radiation. Elemental analysis of the waste materials was performed with X-ray fluorescence technique. Laser diffraction technique was used to determine particle size distribution (Malvern Mastersizer) of the waste particles. The schematics of the preparation of the waste and its characterization are given in Fig. 2.

Preparation of Hybrid Composites

Since the objective of the study was to determine the effect of ceramic particulate to glass fiber ratio and the particle size on the properties, epoxy to waste ratio was kept constant for all of the compositions as 40 to 60 wt%. For the prepared mixtures, the coding described as follows was adopted. The first figure represented the particle size range, F (fine) <90 μm, M (medium) 90–150 μm and C (coarse) 150–300 μm. The rest of the code indicated the ceramic particulate and glass fiber weight ratios, each indicated by two digits, and all added up to 60 wt%. As can be seen from Table 1 composites

TABLE 1. Specifications of prepared hybrid composites.

Code	Ceramic: Glass Fiber ratio (wt%)	Particle size of wastes (μm)
F6000	60:00	<90
F5505	55:05	<90
F5010	50:10	<90
F4020	40:20	<90
M5505	55:05	90–150
M5010	50:10	90–150
M4020	40:20	90–150
C5505	55:05	150–300
C5010	50:10	150–300
C4020	40:20	150–300

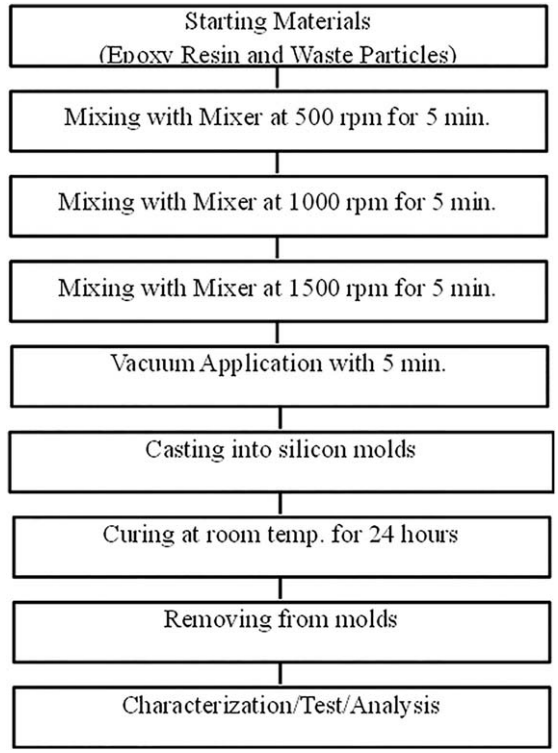

FIG. 3. Composite production process flow chart.

were prepared with waste wall tile particulates ratio in the range 40–55 wt%. The preparation process is given in Fig. 3, schematically.

Polymer matrix composites were produced with the casting method. Before casting, the mold was coated with polyvinyl alcohol (PVA) as lubricant for subsequent easy removal of the composites from the mold. Epoxy resin, hardener and waste particles were blended in a propeller mixer at 500, 1,000, and 1,500 rpm for 5 min at each speed. The purpose of the slow mixing speed in the beginning was to avoid the loss of filler powder by dusting. Once the filler was incorporated into the liquid polymer the mixing rate was increased stepwise to obtain a homogeneous mixture. Vortex formation was avoided to minimize trapped air bubbles. The blended mixture was subjected to vacuum desiccation to remove any existing air bubbles. This was necessary to prevent pores in the composite. The blended mixture was poured into the lubricated silicon molds. The epoxy resin-fillers blend was left for 24 h in the mold at room temperature for curing, and thereafter the epoxy resin hybrid composites were removed from the mold.

Physical, Mechanical, and Microstructural Characterization

To determine the theoretical density of the composite, the theoretical densities of the waste materials and the epoxy resin were used. Theoretical density of composite was calculated from the theoretical densities and the volume fractions

DOI 10.1002/pc

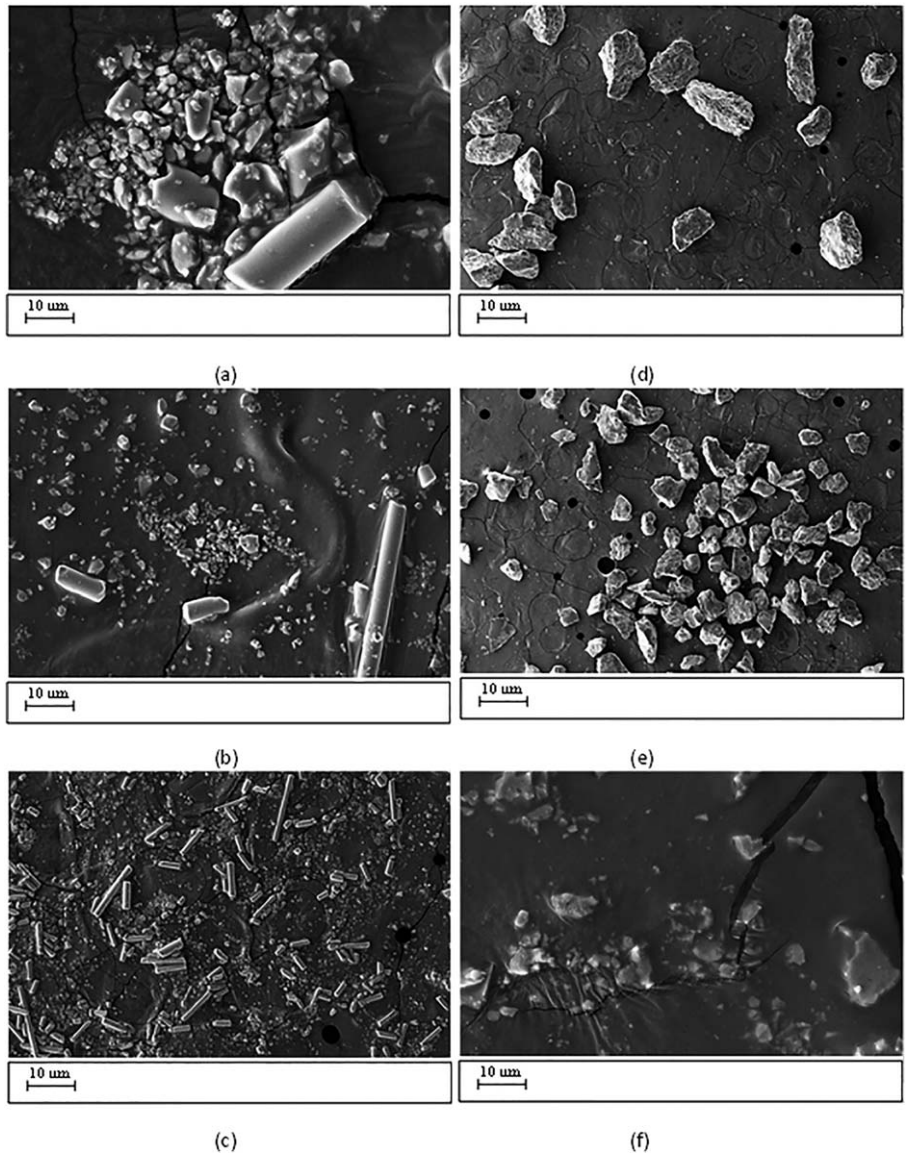

FIG. 4. SEM-SE images of waste particles, (a) glass fiber waste with particle size below 90 μm, (b) between 150 and 300 μm, (c) 300 μm; (d) wall tile waste with particle size below 90 μm, (e) between 150 and 300 μm, (f) 300 μm.

of the constituting materials given by *Eq. 1* [3]. The known weight fractions were converted to volume fractions.

$$\rho_c = \rho_m V_m + \rho_{r1} V_{r1} + \rho_{r2} V_{r2} \quad (1)$$

where, ρ_c is theoretical density of composite, ρ_m is theoretical density of matrix, ρ_{r1} and ρ_{r2} are the theoretical densities of the ceramic powder and glass fiber reinforcements, respectively, while V_m is the volume fraction of the matrix, and V_{r1} and V_{r2} are the volume fractions of the respective reinforcements.

The Archimedes principle was used to measure the density and porosity of the samples. Bulk density, % theoretical density and % total porosity were calculated by *Eqs. 2–4*.

$$\text{Bulk Density} = \frac{W_1}{W_3 - W_2}\rho_{\text{water}}$$

$$\%\text{T.D.} = \frac{\text{BD}}{\text{TD}}100$$

$$\%\,\text{Total Porosity} = 100 - \%\,\text{T.D.}$$

where, W_1 is the dry weight, W_2 is the wet weight suspended in water, W_3 is the wet weight, B.D. is the bulk density, T.D. is the theoretical density of the samples.

The Shore-D hardness was measured with 5 × 5 cm samples. The average of the five measurements was taken. Three point-bending strength tests of the samples were done according to TS 985 EN ISO 178 standard. At least three measurements were used to calculate the bending modulus by *Eq. 5*.

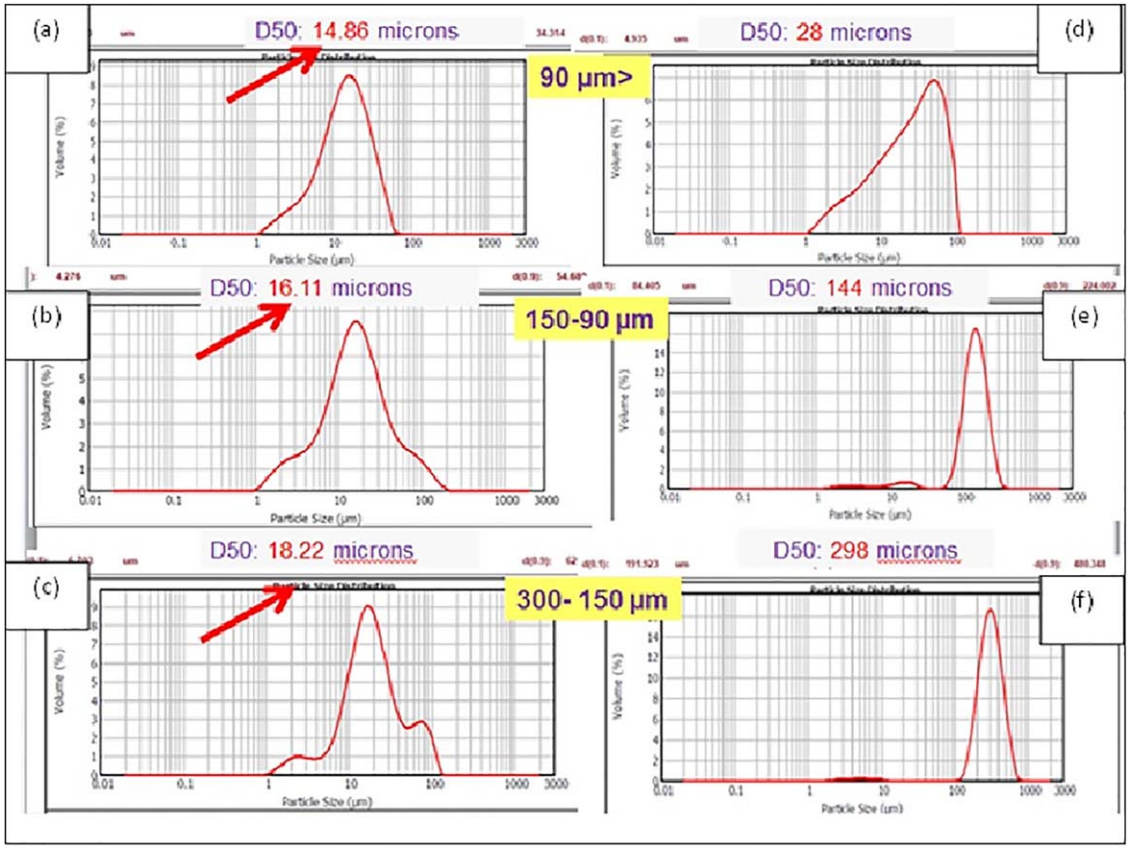

FIG. 5. Particle size distribution graphs of waste particles (a) glass fiber waste with particle size below 90 µm, (b) between 150 and 300 µm, (c) 300 µm; (d) wall tile waste with particle size below 90 µm, (e) between 150 and 300 µm, (f) 300 µm. [Color figure can be viewed at wileyonlinelibrary.com]

$$E = \frac{L^3 m}{4WD^3} \tag{5}$$

where, E is the bending modulus, m is slope, L is the distance between the span, W is the width, and D is thickness of the test sample.

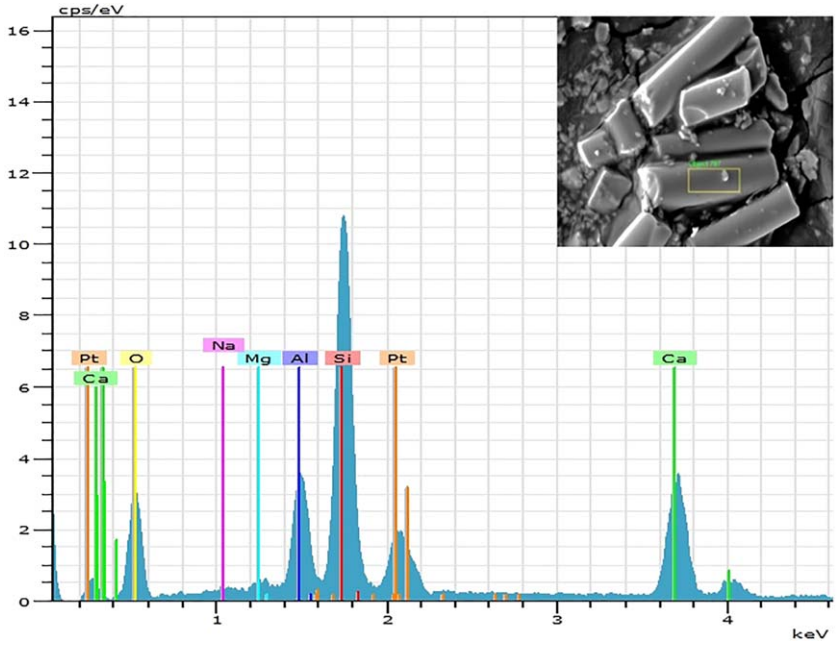

FIG. 6. SEM-EDX analysis of glass fiber waste. [Color figure can be viewed at wileyonlinelibrary.com]

DOI 10.1002/pc

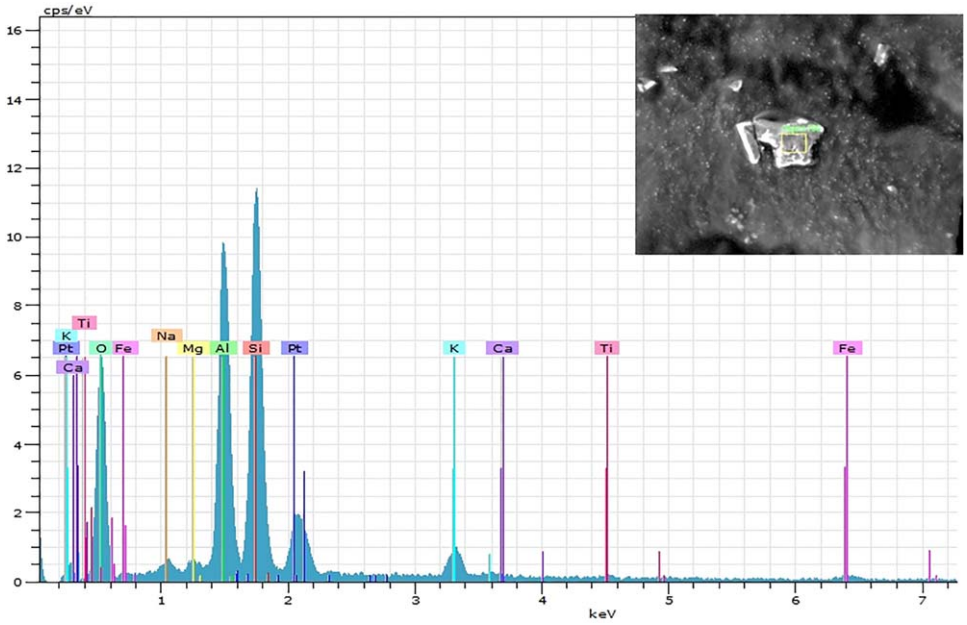

FIG. 7. SEM-EDX analysis of wall tile waste. [Color figure can be viewed at wileyonlinelibrary.com]

The impact resistance of the hybrid composite samples was measured with Devotrans impact test equipment. The tests were performed in accordance with the standard ISO EN 180 U. The samples of sizes 80 × 10 4 mm were subject to the impact of 6J hammer. The results were obtained as the average of 5 measurements. The hammer energy transmitted for the breakage of the sample was calculated by *Eq. 6*.

$$a_{iU} = \frac{E_c}{h \cdot b} \times 10^3 \quad (6)$$

where, E is the transmitted energy in joule (J), h is the sample thickness in mm, b is the sample width in mm, a_{iu} is the impact resistance in kJ/m^2.

The microstructural investigation of the polished and fractured surfaces of samples was performed by scanning electron microscope (SEM-Zeiss Supra 40VP) imaging. The samples to be polished were molded in polyester resin. Secondary electron scanning electron microscopy images of waste materials were taken with Zeiss Supra 40 VP FEG-SEM. The phases were determined by X-ray diffraction analysis (XRD-Panalytical, Empyrean with Cu-Kα radiation). Elemental analysis was performed with the X-ray fluorescence technique.

TABLE 2. XRF analysis result of glass fiber waste.

Element	wt.%	Oxide	wt.%
Si	50.281	SiO2	59.913
Ca	29.987	CaO	20.607
Al	14.212	Al2O3	15.415
Mg	1.51	MgO	1.451
Na	1.037	Na2O	0.815
Ti	0.518	TiO2	0.384

RESULTS AND DISCUSSION

Waste Characterization

Ground waste particles were sieved to obtain particle size distributions in the ranges below 90 μm, between 90 and 150 μm and between 150 and 300 μm. Scanning electron microscopy images of waste glass fiber showed that particles had elongated shape with the aspect ratio changing from 1 to 7. Conversely, the ground waste ceramic particles were of irregular shape over a wide size range (Fig. 4). The particle shape is an important parameter that affects the processability (rheological properties) and a number of mechanical properties of hybrid composites. Glass fiber particle size distributions were given in Fig. 5a–c. The mean particle size in the indicated ranges changed slightly from 14 to 18 μm with broad distributions. However in the 150–300 μm range, the particle size distribution showed two local maxima an above and below the mean particle size (18 μm) due to elongated particle shape. The waste wall tile particle size distributions are shown in Fig. 5d–f. The results showed that mean particle size changed from 30 to 300 μm, and while

TABLE 3. XRF analysis result of wall tile waste.

Element	Wt.%	Oxide	Wt.%
Si	65.987	SiO2	71.836
Al	18.562	Al2O3	18.633
K	5.395	K2O	2.903
Na	2.964	Na2O	2.17
Ti	1.121	TiO2	0.806
Ca	0.887	CaO	0.542
Mg	0.663	MgO	0.59

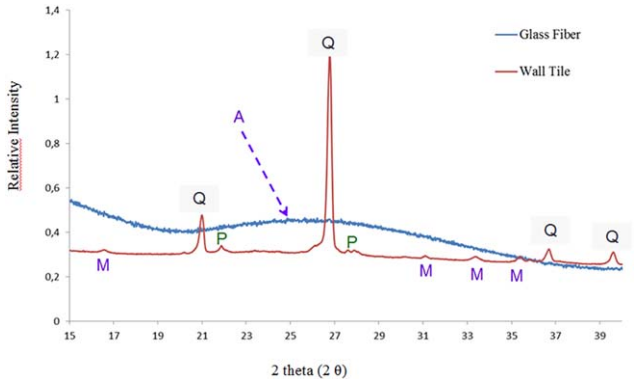

FIG. 8. XRD graphs of waste materials (A: Amorphous Silica; Q: Quartz; P: Plajioklas; M: Mullite). [Color figure can be viewed at wileyonlinelibrary.com]

the range below 90 μm showed a broader particle size distribution, in the other ranges the distributions were narrower.

Elemental analyses of waste materials were performed by scanning electron microscope with the EDX detector. Si, Ca, and O were the main elements in the waste glass fiber sample with little amounts of Al and Mg (Fig. 6). The results showed that the waste material consisted of SiO_2, CaO, Al_2O_3 and little amount of MgO. Conversely, Si, Al, and O are primary elements in wall tile waste and hence SiO_2 and Al_2O_3 were basic constituents (Fig. 7). Minor amounts of K_2O, Fe_xO_y, Na_2O, MgO, and TiO_2 were present in the waste wall tile sample. The source of the Pt peak was regarded as the sputter coated Pt for conduction.

The results of XRF analyses of the waste materials are shown in the Tables 2 and 3. SiO_2, CaO, Al_2O_3 were the main constituents in the glass fiber waste. Minor amounts of MgO, Na_2O and TiO_2 were available (Table 2). Wall tile waste composed of mainly SiO_2 and Al_2O_3 oxides with little amounts of K_2O, Na_2O, TiO_2, CaO, and MgO (Table 3).

Figure 8 represents the XRD pattern of waste materials. The very broad peak in glass fiber XRD pattern indicated that the main phase of glass fiber was amorphous silica. Conversely, in the waste wall tile samples quartz was the main phase with small amount of plagioclase, a mixture of albite and anorthite phases, and mullite.

TABLE 4. Bulk density, theoretical density, % theoretical density and %total porosity of hybrid composites.

Samples	Bulk Density	%Total Porosity	Theoritical Density	%Theoritical Density
F5505	1,60	20,75	2,019	79,25
F5010	1,58	21,82	2,021	78,18
F4020	1,57	22,51	2,026	77,49
M5505	1,57	22,24	2,019	77,76
M5010	1,55	23,31	2,021	76,69
M4020	1,52	24,98	2,026	75,02
C5505	1,54	23,72	2,019	76,28
C5010	1,56	22,81	2,021	77,19
C4020	1,55	23,49	2,026	76,51

TABLE 5. Shore-D hardness values of hybrid composites.

	Shore D Hardness	Particle size (μm)	%Total Porosity	%Theoritical Density
Epoxy	80.50 ± 4.9			
F6000	96,33 ± 0,44	90>	22,16	77,84
F5505	94,50 ± 1.00	90>	20,75	79,25
F5010	93,00 ± 1,50	90>	21,82	78,18
F4020	92,13 ± 0,88	90>	22,51	77,49
F0060	91,50 ± 1,00	90>	21,76	78,24
M5505	92,00 ± 0,80	90–150	22,24	77,76
M5010	91,16 ± 0,78	90–150	23,31	76,69
M4020	90,00 ± 0,10	90–150	24,98	75,02
C5505	90,33 ± 0,44	150–300	23,72	76,28
C5010	89,50 ± 1,50	150–300	22,81	77,19
C4020	88,33 ± 0,89	150–300	23,49	76,51

Physical Properties of Composites

Table 4 shows the bulk density, theoretical density, % theoretical density and vol.% total porosity of the composites. The bulk density values of composite materials changed between 1.52 for M4020 to 1.60 gr/cm^3 for F5505. % total porosity values changed between 20,75% for F5505 to 24,98% for M4020 composites. Increase in bulk density was accompanied by a decrease in % total porosity and an increase in % theoretical density.

Composites produced with the filler particles in the finest range (<90 μm) yielded higher bulk density values. Conversely, the increase in glass fiber content resulted in lower bulk density and higher porosity and hence yielded lower theoretical densities. Addition of glass fiber might have worsened the processability of the mixture due to the relatively high aspect ratio. In our previous study the highest bulk density and the lowest total porosity were achieved with waste particle size which was around 150 μm [19]. If the particle size was below 45 μm, the particles had higher surface area and processability was worse). Therefore, a composite consisting of fine particles caused higher porosity, and the % theoretical density decreased. Acikbas et al. used porcelain waste in epoxy matrix and the results showed that a higher bulk density was achieved with the waste particle size below 90 μm as compared to waste particles in the size range of 90–150 μm and 150–250 μm [18].

Shore-D Hardness

The Shore-D hardness results of the hybrid composites are given in Table 5. Addition of waste particles into epoxy resin caused an increase of the hardness of the monolithic epoxy resin. The hardness increased only slightly with the use of the finer particles (<90 μm). However with the addition of the fillers in the other size ranges the hardness was not affected appreciably.

DOI 10.1002/pc

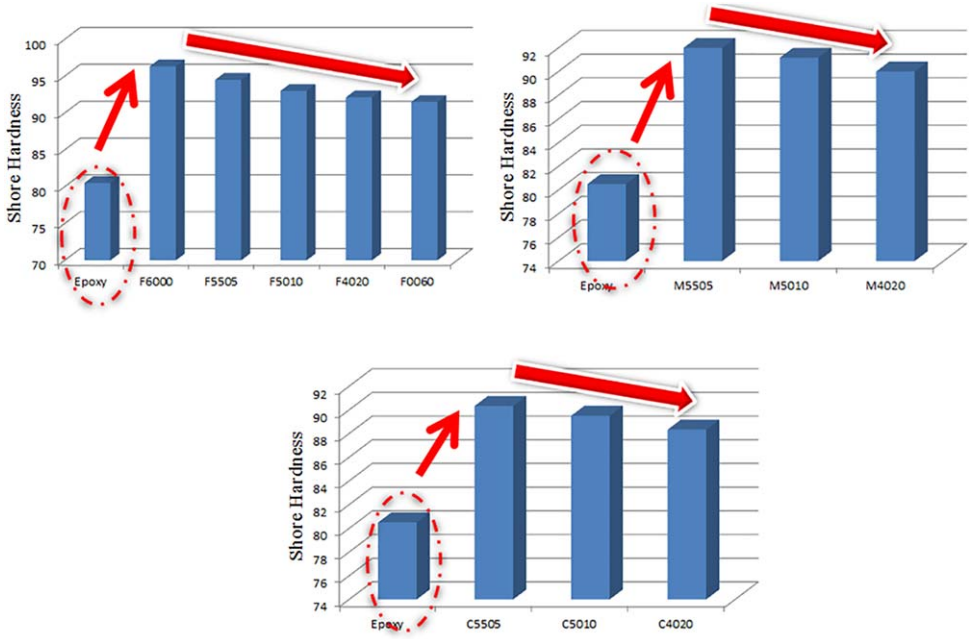

FIG. 9. The effect of ceramic:fiber ratio on hardness of hybrid composites. [Color figure can be viewed at wileyonlinelibrary.com]

Increase in the glass fiber content led to a decrease in the hardness for all particle size ranges which was related to matrix-reinforcement interphase bonding (Fig. 9). Since the glass fibers had smoother surface (Fig. 10a) than the wall tile waste, interphase bonding would be weaker. Therefore lower hardness values were obtained with the increase in glass fiber content as seen from the C4020 composition which was rich in glass fiber (Fig. 10c). Because wall tile waste had rough surfaces (Fig. 10b) and hence higher surface area, connectivity between the matrix and filler was strong as seen from C5505 composition (Fig. 10d).

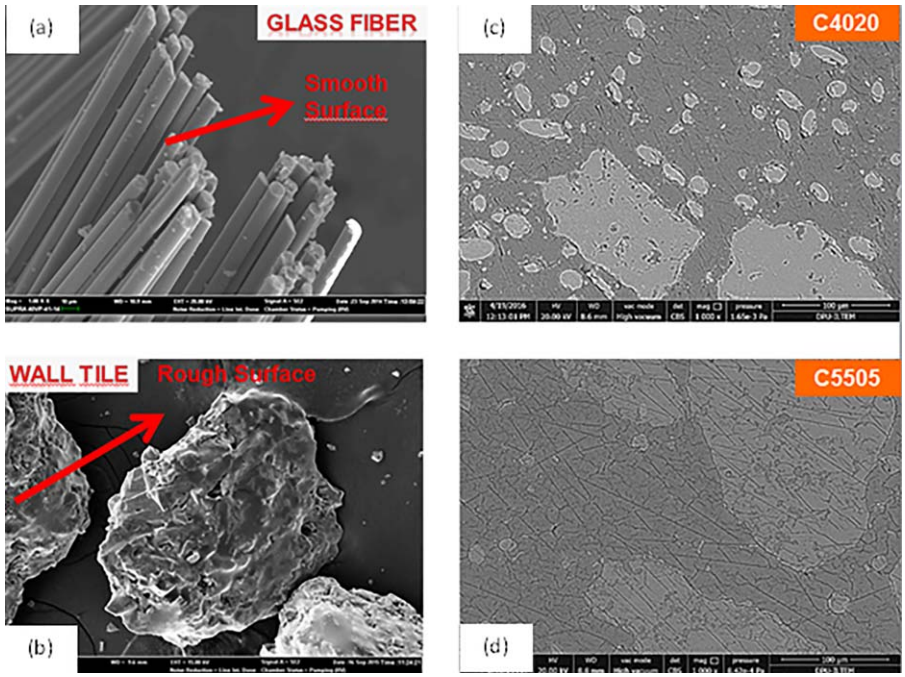

FIG. 10. SEM images of (a) the glass fiber, (b) the wall tile waste, (c) C4020, (d) C5505. [Color figure can be viewed at wileyonlinelibrary.com]

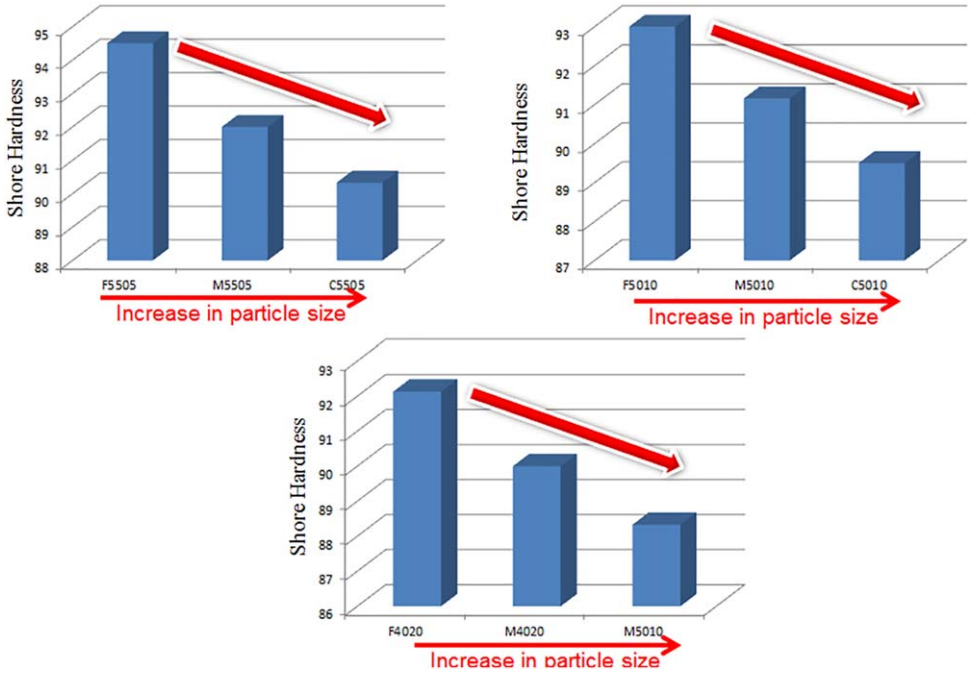

FIG. 11. Effect of particle size on hardness of hybrid composites. [Color figure can be viewed at wileyonlinelibrary.com]

The hardness affected by porosity and matrix-reinforcement interphase bond strength. The porosity values obtained from Archimedes principle changed between 20,75% and 24,98% for hybrid composites which were produced with particles in all of the size ranges. Increase in porosity led to a decrease in hardness values. F5505 composite with 20,75%TP had 94,5 Shore-D hardness while C5505 composite with 23,75%TP had 90,33 Shore-D hardness.

Conversely, waste particle size affected the matrix-reinforcement interphase bonding. If the particles were

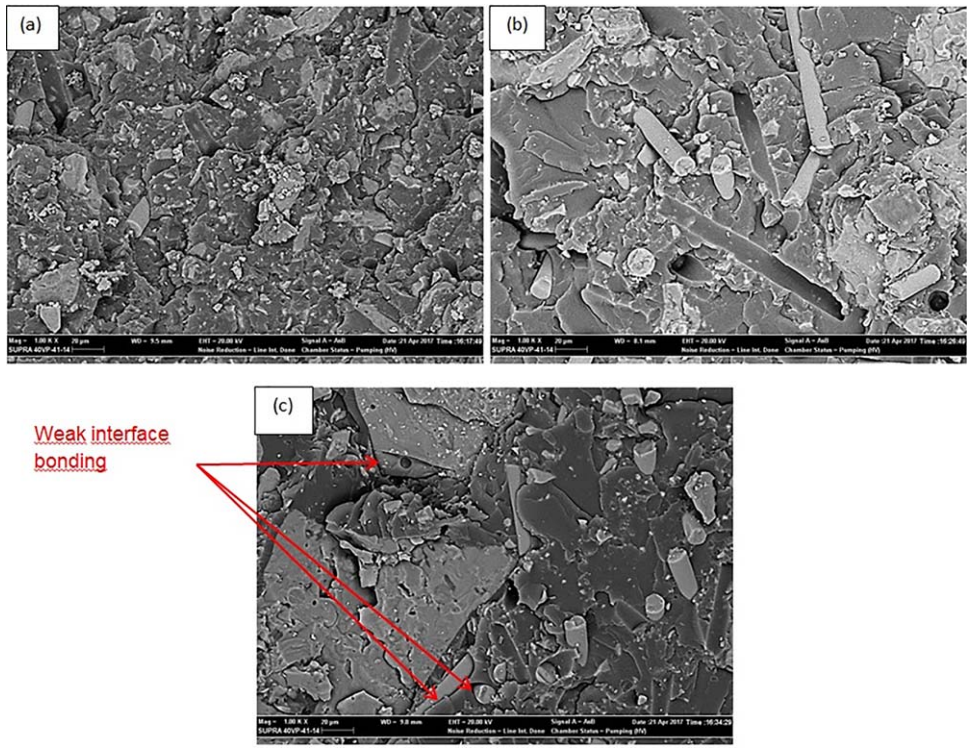

FIG. 12. Representative SEM images of hybrid composites contains different particle sizes (a) F5010, (b) M5010, and (c) C4020. [Color figure can be viewed at wileyonlinelibrary.com]

DOI 10.1002/pc

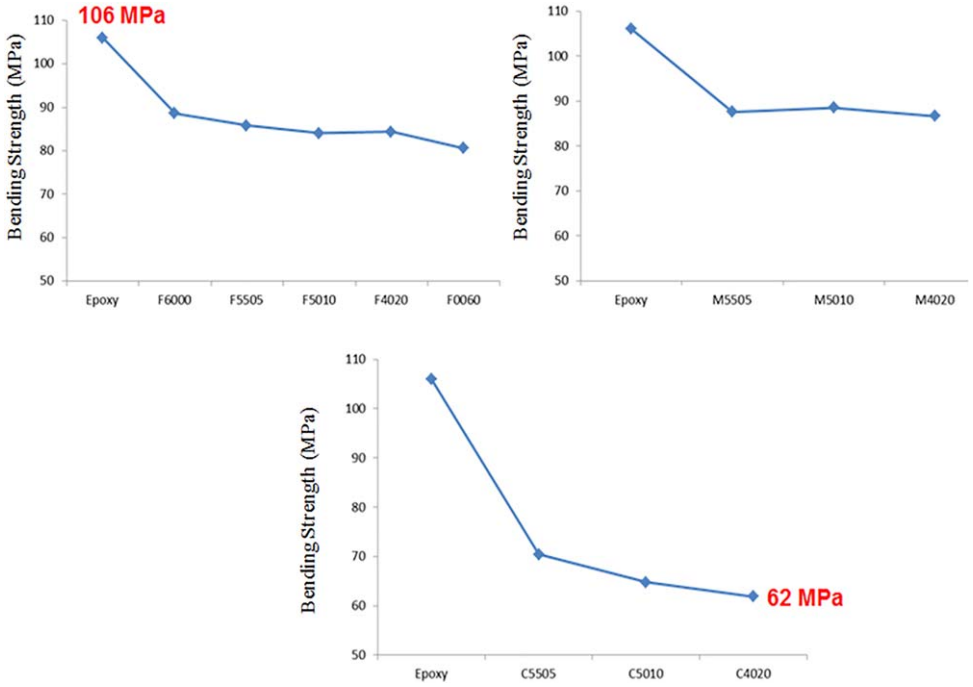

FIG. 13. The effect of ceramic:fiber ratio on bending strength of hybrid composites. [Color figure can be viewed at wileyonlinelibrary.com]

finer, matrix-reinforcement interphase bonding would be strong since fine particles had higher surface roughness and hence provided stronger interphase bonding, and hence better hardness values were achieved (Fig. 11). SEM images of hybrid composites with particles in different size ranges are given in Fig. 12. As seen from the SEM images matrix-reinforcement interphase bonding was weaker when particles in the coarser size ranges. F5010 composition showed better interphase bonding and with the increase in particle size, interphase bonding became weaker for M5010 and C5010 compositions.

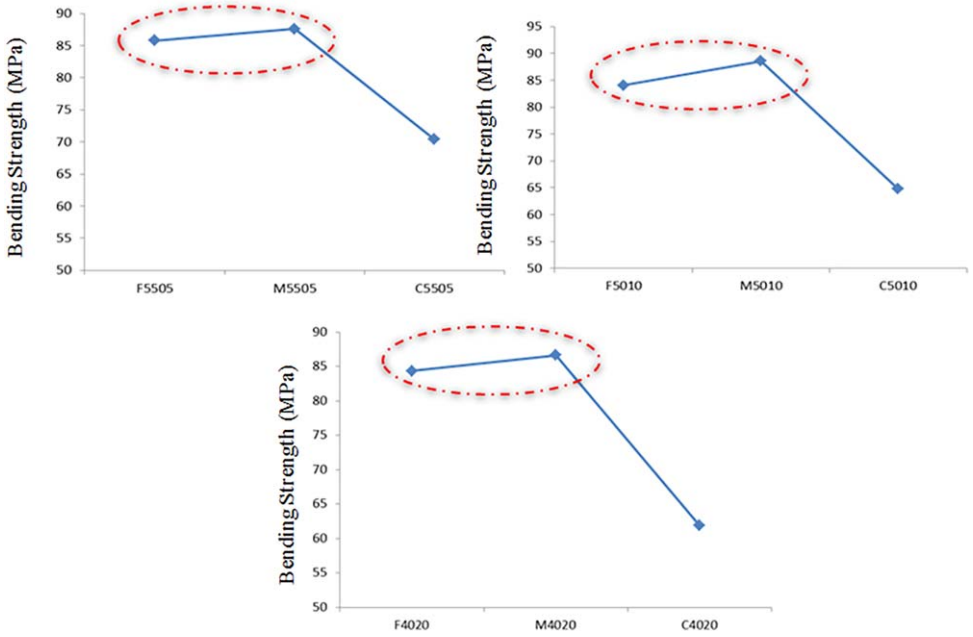

FIG. 14. Effect of particle size on bending strength of hybrid composites. [Color figure can be viewed at wileyonlinelibrary.com]

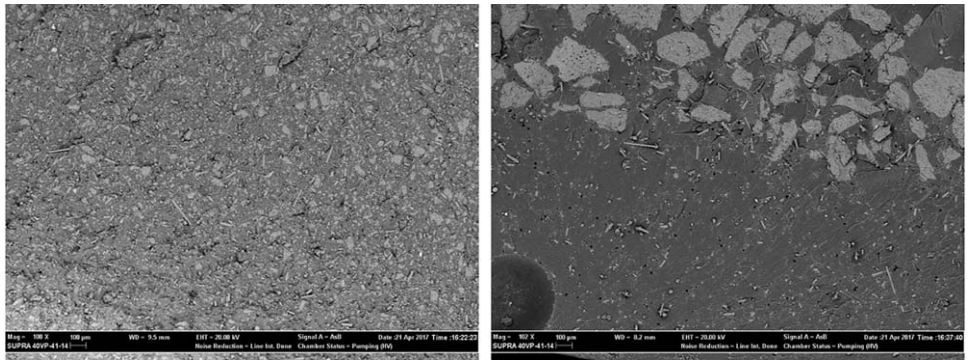

FIG. 15. SEM-BSE images of (a) F5010 and (b) C5505.

Bending Strength and Bending Modulus

Bending strength values changed between the 106 MPa for the epoxy matrix to 62 MPa for C4020 composition. Addition of waste particles into epoxy resin led to a decrease in bending strength due to the brittleness induced by the filler. Conversely with the increase in glass fiber amount, bending strength decreased because of the weak interphase bonding. The same phenomenon was observed for particles in all of the size ranges (Fig. 13). F6000 composite which was reinforced only by ceramic particulates yielded a bending strength of 88,6 MPa, whereas for the F5505 hybrid composite obtained with the addition of 5wt% glass fiber waste showed a slightly lower bending strength which was 85,8 MPa. Addition of glass fiber weakened the matrix-reinforcement interphase and so lowered the bending strength. The maximum bending strength value of 88,55 MPa was obtained for M5010. The minimal bending strength of 61,90 MPa was obtained for C4020 which consisted of particles in the coarser range (150–300 μm) and with the highest glass fiber content. The addition of glass fibers caused a resistance for the homogeneous distribution of particles in matrix lowering bending strength.

When the particle sizes in the ranges below 90 μm and between the 90–150 μm, the bending strength did not change with ceramic:fiber ratio (Fig. 14). However, in the particle size range 150–300 μm, bending strength decreased with the increasing ceramic:fiber ratio. This could have been resulted because of the lower interphase bond strength and non-homogenous distribution of waste particles in the epoxy matrix. With the finer particle sizes distribution of particles in the matrix was more homogeneous as revealed with the higher bending strength values were obtained (Fig. 15). From the SEM-BSE images of F5010 and C5505

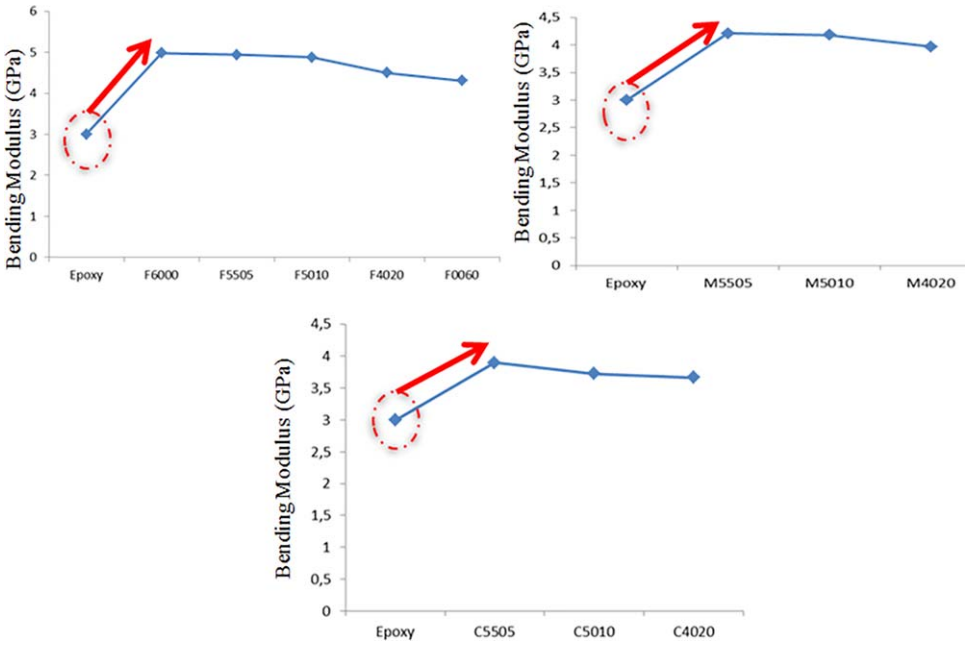

FIG. 16. Effect of ceramic:fiber ratio on bending strength of hybrid composites. [Color figure can be viewed at wileyonlinelibrary.com]

DOI 10.1002/pc

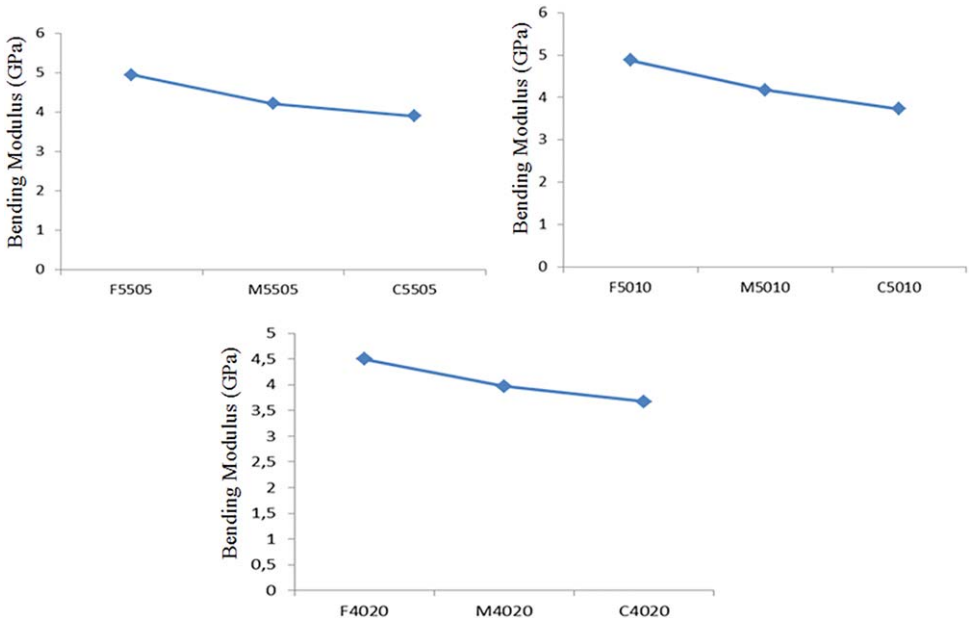

FIG. 17. Effect of particle size on bending modulus of hybrid composites. [Color figure can be viewed at wileyonlinelibrary.com]

composites, it seemed that segregation problem and inhomogeneous distribution of filler particles were resulted with the use of the coarse ceramic particles which were heavier than the glass fibers. Therefore, during mixing heavy particles sinked to the bottom and led to inhomogeneity in the composite structure. Besides, an increase in filler particle size led to a decrease in filler volume in the composite. Calis-Acikbas and Acikbas showed that urea formaldehyde waste containing composites showed an increase in bending strength from 65,25 MPa to 91,52 MPa with the particle size increased from below 45 μm to above 150 μm. The results revealed that in the particle size range of 90–150 μm the reinforcement was effective obtaining higher bending strength values [19].

Bending modulus improved with the addition of reinforcement fillers into epoxy resin (Fig. 16). Incorporation of glass fibers, in any of the size ranges in the composite, deteriorated the bending modulus only slightly. The

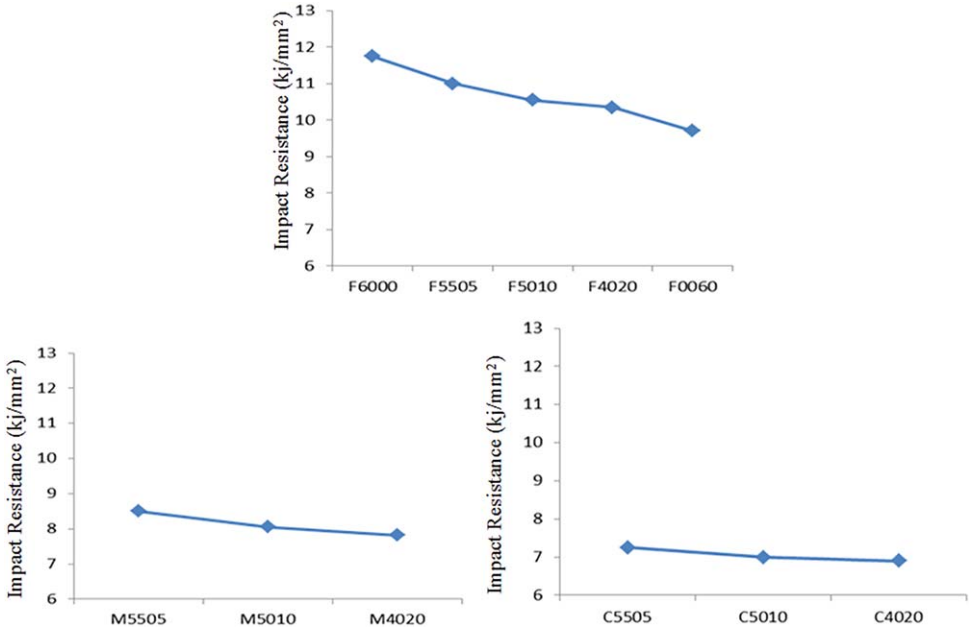

FIG. 18. Effect of ceramic:fiber ratio on impact resistance of hybrid composites. [Color figure can be viewed at wileyonlinelibrary.com]

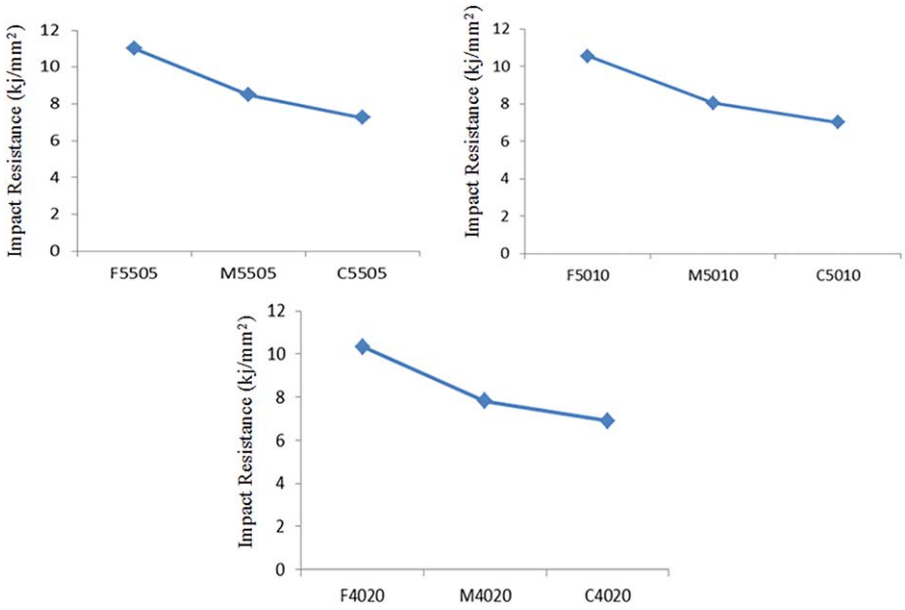

FIG. 19. Effect of particle size on impact resistance of composite of hybrid composites. [Color figure can be viewed at wileyonlinelibrary.com]

increase in particle size was accompanied with a decrease in bending modulus due to weak interphase bonding (Fig. 17).

Impact Resistance

The increase in glass fiber content led to weaker interphase bonding, and hence, caused deterioration of the impact resistance for all particle size ranges. For the filler particle size range of <90 μm the decrease was from 11.75 to 9.75 kJ/mm^2, for the size range of 90–150 μm it was from 8.50 to 7.82 kJ/mm^2, and for the size range of 150–300 μm it was from 7.25 to 6.90 kJ/mm^2 (Fig. 18). Also, the increasing particle size caused weaker interphase bonding lowering the impact resistance (Fig. 19).

CONCLUSIONS

The characterization of waste particles was performed with different characterization tools. The waste glass fiber had smooth surfaces which in turn caused a weak epoxy matrix-filler interphase bonding. The waste wall tile particles provided stronger interphase bonding with the matrix, affecting the mechanical properties of hybrid composite positively. Theoretical densities of the glass fiber and wall tile powder were 2.61 gr/cm^3 and 2.54 gr/cm^3, respectively. XRF and EDX analyses showed that the waste glass fiber was mainly composed of SiO_2, CaO and Al_2O_3, while the waste wall tile was composed of SiO_2 and Al_2O_3. XRD analysis revealed that glass fiber had amorphous silica phase, and wall tile consisted of quartz as the primary phase with plagioclase and mullite phases present in minor amounts.

Bulk density values of hybrid composites were nearly the same and changed between 1.52 gr/cm^3 and 1.60 gr/cm^3. Addition of hard particles into epoxy matrix caused increase in hardness, bending modulus and decrease in bending strength. F5505 was the optimum composition in terms of high theoretical density, hardness, bending strength, bending modulus and impact resistance. With the increase in fiber ratio, bulk density, hardness, bending strength and impact resistance were adversely affected. Increase in particle size led to decrease in bulk density, hardness, bending strength, bending modulus and impact resistance. Incorporation of glass fiber waste deteriorated the physical and mechanical properties due to the weak matrix-filler interphase bonding. These composites are candidates for sanitaryware applications (e.g., sink, bench, closet. . ..) since they combine the required properties of lightness, high impact resistance, convenience for the production of complex shapes and being eco-friendly in contrast to conventional ceramic sanitaryware. As a result, incorporation of glass fiber and wall tile wastes basically resulted in the reinforcement of the epoxy matrix. This allows for the recycling of inorganic ceramic residues as well as improving some mechanical properties of the composites.

ACKNOWLEDGEMENT

The supply of the waste materials by the companies Şişecam Glass Fiber A.Ş. (Gebze, Turkey) and Bien Ceramic (Bilecik, Turkey) was gratefully acknowledged.

REFERENCES

1. B.V. Perov and I.P. Khoroshilova, "Polymer Matrix Composites: Hybrid composite materials, Volume 4, Soviet Advanced Composites Technology Series, 269–304," Springer Netherlands (1995).

DOI 10.1002/pc

2. C.-S. Kim, C. Randow, T. Sano, *Hybrid and Hierarchical Composite Materials*, Switzerland, Springer International Publishing, (2015).
3. B. Harris, *Engineering Composite Materials*, The Institute of Materials, London (1999).
4. B. J. Hunt, J. B. Howes, G. Hunt, Waste Reduction Programs for Commercial/Industrial Solid Waste, http://citeseerx.ist.psu.edu/viewdoc/download?doi=10.1.1.399.2000&rep=rep1&type=pdf
5. A. Ashori, *J. Polym. Environ.*, **18**, 65 (2010).
6. R.O. Medupin, O.K. Abubakre, O. Ukoba, and P.E. Imoisili, *Am. Chem. Sci. J.*, **3**, 507 (2013).
7. M. Koleva, A. Zheglova, E. Fidancevska, V. Vassilev, *Composites Containing Waste Materials*, INTECH Open Access Publisher (2011).
8. M. Sathiyamoorthy, S. Thanappan, and M. Senthilkumar, *Int. J. Eng. Res. Ind. Appl.*, **4**, 335 (2011).
9. M. Tunsan, *Waste Manage. Res.*, **21**, 83 (2003).
10. V. Vassilev, E. Fidancevska, M. Milosevski, S. Parvanov, D. Milosevski, and T. Hristova- Vasileva, *J. Univer. Chem. Technol. Metallurg.*, **42**, 369 (2007). VolNo.4, ISSN 1311–7629.
11. C. Thomas, P.H.R. Borges, T.H. Panzera, A. Cimentada, and I. Lombillo, *Compos. Part B*, **59**, 260 (2014).
12. S. Alok and P. Amar, *J. Reinf. Plast. Comp.*, **29**, 1 (2008).
13. M.R. Parvaiz, S. Mohanthy, S.K. Nayak, and P.A. Mahanwar, *J. Miner. Mater. Char. Eng.*, **9**, 25 (2010).
14. S. Biswas, A. Satapathy, and A. Patnaik, *Adv. Mater. Res.*, **123–125**, 1031 (2010).
15. N.V. Kumar, M.M.M. Sarcar, K. Ramji, and V. Geetha, *Int. J. Theor. Appl. Res. Mech. Eng.*, **3**, 2319 (2014).
16. P. Mishra and T. Bera, *Int. J. Adv. Res.*, **2**, 122 (2014).
17. J.O. Agunsoye, S.I. Talabi, E.O. Obidiegwu, and I.O. Awe, *Int. J. Compos. Mater.*, **4**, 93 (2014).
18. G. Acikbas, N. Calis Acikbas, E. İkizek, M. Özel, E A.S. Eker, Characterization of green epoxy matrix composites filled with ceramic wastes. ISITES2014 2nd International Symposium on Innovative Technologies in Engineering and Science Proceeding Book, 597–606, 18–20 June, 2014, Karabük, Turkey.
19. N. Calis Acikbas and G. Acikbas, *Waste Biomass Valorization*, **8**, 669 (2017).
20. G. Acikbas, Development and characterizatıon of polymer matrix composite materials alternative to ceramic sanitarywares. Materials Science and Engineering, Ph.D. Thesis, 2016, Dumlupinar University, Turkey.
21. K. Ahmed, S.S. Nizami, and N.Z. Riza, *J. Adv. Res.*, **5**, 165 (2014).
22. M.M. Thwe and K. Liao, *Compos. Sci. Technol.*, **63**, 375 (2003).
23. M. Haneef, F. Rahman, M. Yunus, S. Zameer, S. Patil, and T. Yezdani, *Int. J. Modern Eng. Res.*, **3**, 970 (2013).
24. M.R. Sanjay and B. Yogesha, *J. Miner. Mater. Char. Eng.*, **4**, 15 (2016).
25. M. Valente, F. Sarasini, F. Marra, J. Tirillò, and G. Pulci, *Compos. Part A*, **42**, 649 (2011).
26. Sh, K. Amin, H.A. Sibak, S.A. El–Sherbiny, and M.F. Abadir, *Int. J. Appl. Eng. Res.*, **11**, 2680 (2016).
27. www.thetiledoctor.com/tile